Available online at www.sciencedirect.com
ScienceDirect
Journal of Sound and Vibration 311 (2008) 667–682
JOURNAL OF SOUND AND VIBRATION
www.elsevier.com/locate/jsvi

# Study on free vibration analysis of circular cylindrical shells using wave propagation

Li Xuebin

*Wuhan 2nd Ship Design and Research Institute, Wuhan, Hubei Province, 430064, People's Republic of China*

Received 2 November 2006; received in revised form 18 September 2007; accepted 23 September 2007
Available online 26 October 2007

**Abstract**

A wave propagation approach is presented for free vibration analysis of circular cylindrical shell, based on Flügge classical thin shell theory. The validity and accuracy of the wave approach is studied in detail, including aspects of frequencies, vibration shapes and wavenumbers. An exact solution for free vibration of circular cylindrical shell is also given in the present analysis. For the comparisons of these two approaches for natural frequencies, vibration shape of a shell are discussed for shear diaphragm–shear diaphragm (SD–SD), clamped–clamped (C–C) and clamped–shear diaphragm (C–SD) boundary conditions. The results show that wave propagation has high accuracy for long shell and SD–SD boundary conditions.


## 1. Introduction

Of all existing shell models, the circular cylindrical shell is perhaps the most widely studied. It has applications in chimney design, pipe flow and aircraft fuselages to name a few. Many shell theories have been developed over the last century, as well as methods to solve their governing equations. A comprehensive review and comparison of shell theories have been carried out by Leissa [1]. The free vibration and wave problems of thin circular cylindrical shells have been of great interest to many structural engineers in recent years. They used so many approaches in their research. Fuller [2] studied the effects of wall discontinuities on the propagation of flexural waves in cylindrical shells. The transmission of flexural-type wave through various discontinuities in the walls of cylindrical shells is investigated. Theoretical curves of transmission loss are obtained for different circumferential wavenumbers and wave types, as functions of frequency. The dispersion behavior and energy distributions for free waves in thin-walled cylindrical shells filled with fluid are studied by Fuller and Fahy [3]. Fuller [4] has investigated the input mobility of an infinite circular cylindrical shell. Wang and Lai [5] introduced the wave propagation approach to study the vibration behavior of finite-length circular cylindrical shells based on Love's shell theory, and an approximate method for calculating the natural frequencies of finite-length circular cylindrical shells with different boundary conditions without simplifying the exact equations of motion. Those approximate solutions are compared with numerical results obtained using finite-elements code ANSYS and with experimental data. Zhang et al. [6] studied the vibration

*E-mail address:* li_xuebin@163.com

0022-460X/$ - see front matter © 2007 Elsevier Ltd. All rights reserved.
doi:10.1016/j.jsv.2007.09.023

**Nomenclatures**

| | |
|---|---|
| $a_i$ | coefficients of characteristic equations |
| $b_i$ | coefficients of characteristic frequency equations |
| $C$, $A$ | frequency matrix of wave propagation and exact solution, respectively |
| $E$, $v$ | Young's modulus and Poisson's ratio |
| $h$, $R$, $L$ | thickness, radius and length of shell |
| $k_m$ | wavenumber in the axial direction (wave propagation) |
| $n$ | circumferential wavenumber |
| $u$,$v$,$w$ | axial, circumferential and radial displacement |
| $x$, $\theta$, $z$ | axial, circumferential and radial coordinates |
| $t$ | time |
| $\alpha$, $\beta$ | modal shape coefficients |
| $\lambda$ | wavenumber in axial direction (exact solution) |
| $\omega$ | radial frequency of shell |
| $\rho$ | mass density |
| $\Omega$ | nondimensional frequency parameter |

characteristics of thin cylindrical shells using wave propagation. They calculated the frequencies of a longer shell ($L/R = 20$), and compared the results by the wave propagation method and numerical FEM (MSC/NASTRAN). Zhang et al. have extended this approach for coupled vibration of fluid-filled shells [7], submerged shells [8] and cross-ply laminated composite shells [9]. Xu et al. studied the power flow propagating in fluid-filled shells [9–13].

As we all know, the accuracy of FEM results is dependent on the number of mesh elements and nodes. The FEM results should be validated itself first. This procedure is very tedious, especially for parametric analyses, for example, if we need to obtain the natural frequencies of shell for different thickness, length–radius ratios and use results are referenced. One kind of meshing may be fine for one length–radius ratio, but may introduce large errors for another ratio. The comparison between wave propagation and exact solution should be made, and then the validity and accuracy of the wave approach could be better evaluated.

In the literature, methods often used to treat cylindrical shells with different boundary conditions include the state-space concept approach [24] and a numerical approach in which one first assumes an unknown axial mode function [15,16]. In all these methods, the natural frequency is first assumed and an iterative procedure is adopted to ensure that the assumed frequency produces a zero of the appropriate characteristic determinant for the particular set of boundary conditions. These methods are therefore highly iterative and computationally intensive. But they have high accuracy. In this paper a wave propagation approach is presented for free vibration analysis of circular cylindrical shell, based on Flügge, classical thin shell theory. The present method of treating cylindrical shells with different boundary conditions by using beam functions as the axial modal functions is a much more straightforward approach. Being a non-iterative method, it is relatively less computationally intensive and it also gives reasonably accurate natural frequencies, at least for simple modal shapes. This approach is also used by other researchers [5,6]; however, the accuracy of this approach is not obtained yet. The validity and accuracy of the wave approach is studied in detail in this analysis, including aspects of frequencies, vibration shapes and wavenumbers. An exact solution for free vibration of circular cylindrical shell is also given simultaneously in this paper. The comparisons of these two approaches for natural frequencies, vibration shape of a shell are discussed for different shells with shear diaphragm–shear diaphragm (SD–SD), clamped–clamped (C–C) and clamped–shear diaphragm (C–SD) boundary conditions. The results show that wave propagation has high accuracy for long shell and SD–SD boundary conditions.

In this paper, a typical dispersion plot is also obtained using the wave propagation approach. From the dispersion plot, one can study more characteristics of the shell itself in view of the wave propagation method.

## 2. Equations of motion of shell

The cylindrical shell under consideration has a constant thickness $h$, radius $R$ and length $L$. The reference surface of the shell is taken at its middle surface where an orthogonal coordinate system ($x$, $\theta$, $z$) is fixed. The $x$

coordinate is taken in the axial direction of the shell, where $\theta$ and $z$ are, respectively, in the circumferential and radial directions of the shell as shown in Fig. 1. The displacements of the shell are defined by $u$, $v$ and $w$ in the $x$, $\theta$ and $z$ directions, respectively. The circumferential modal shapes of shell are shown in this figure (refer to the list of nomenclatures).

The governing differential equations of cylindrical shells based on Flügge [14] can be expressed as

$$\begin{bmatrix} L_{11} & L_{12} & L_{13} \\ L_{21} & L_{22} & L_{23} \\ L_{31} & L_{32} & L_{33} \end{bmatrix} \begin{Bmatrix} u \\ v \\ w \end{Bmatrix} = \{0\}, \tag{1}$$

where $L_{ij}$ $(i,j = 1,2,3)$ are the differential operators with respect to $x$ and $\theta$. The displacements of the shell can be expressed in the form of wave propagation as follows:

$$\begin{aligned} u &= U_m e^{-ik_m x}\cos(n\theta)e^{i\omega t}, \\ v &= V_m e^{-ik_m x}\sin(n\theta)e^{i\omega t}, \\ w &= W_m e^{-ik_m x}\cos(n\theta)e^{i\omega t}, \end{aligned} \tag{2}$$

where $k_m$ and $n$ are axial wavenumber and circumferential modal parameter, respectively, $U_m$, $V_m$ and $W_m$ are, respectively, the wave amplitudes in the $x$, $\theta$ and $z$ directions, $\omega$ is the circular driving frequency. By substituting Eq. (2) into Eq. (1), we obtain

$$\begin{bmatrix} C_{11} & C_{12} & C_{13} \\ C_{21} & C_{22} & C_{23} \\ C_{31} & C_{32} & C_{33} \end{bmatrix} \begin{Bmatrix} U_m \\ V_m \\ W_m \end{Bmatrix} = \{0\}, \tag{3}$$

in which $C_{ij}$ $(I = 1,2,3)$ are coefficients. For the non-trivial solution, the determinant of this set of equations must be zero, i.e.

$$\det([C_{ij}]) = 0, \quad i,j = 1,2,3. \tag{4}$$

A characteristic equation is obtained from the expansion of Eq. (4)

$$f(\lambda,\omega) = 0. \tag{5}$$

Eq. (5) can be rewritten as the following polynomial function; if an initial driving frequency is given:

$$a_8 k_m^8 + a_6 k_m^6 + a_4 k_m^4 + a_2 k_m^2 + a_0 = 0 \tag{6}$$

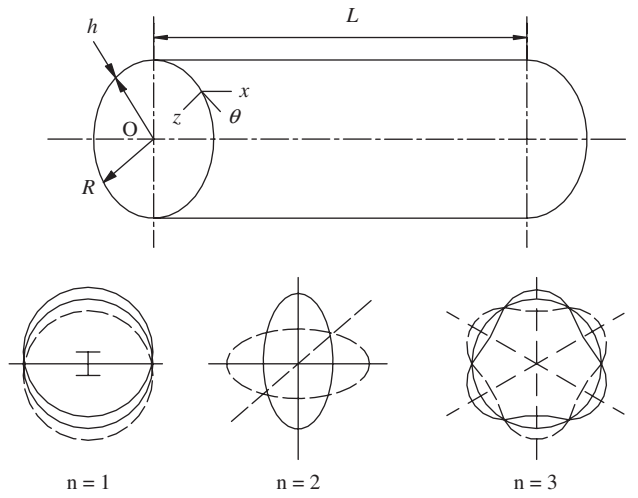


Fig. 1. Coordinate system and circumferential modal shapes.

$a_i$ ($i = 0, 2, 4, 6, 8$) are real coefficients. This is an equation about $k_m$ of order 8. The admissible solutions for a quadric equation with real coefficients consist of combinations or four of $\pm\Lambda_m$, $\pm i\gamma_m$ and $\pm(\psi \pm i\phi)_m$. With the first two types of root, the real and purely imaginary wavenumbers, one obtains propagating wave and an evanescent near field, respectively.

In order to calculate the natural frequencies, it is only necessary to determine the wavenumber $k_m$ in the axial direction. Unfortunately, as $k_m$ strongly depends on the boundary conditions, one has to solve the equations of motion with appropriate boundary conditions in order to obtain $k_m$. However, if one is only interested in flexural vibration, one may use the beam function to determine the modal wavenumbers and mode shapes of cylindrical shells in the axial direction by assuming the flexural mode shapes of cylindrical shells in the axial direction to be of the same form as that of a transverse vibration beam of the same boundary conditions. The key procedure in wave propagation for free vibration analysis of shell is choosing the right shell theory and the right wavenumber in the corresponding beam. After a wavenumber is selected for a given boundary condition, the characteristic equation of the shell becomes

$$\omega^6 + b_4\omega^4 + b_2\omega^2 + b_0 = 0, \tag{7}$$

where $b_i$ ($i = 0, 2, 4$) are coefficients of Eq. (7). This equation governs the characteristics of wave propagation in the shell. There are three roots in this equation, in which the lowest of these three roots represent the flexural vibration; the other two are in-plane vibrations respectively.

The accuracy of wave propagation in free vibration analysis of shell depends on beam's wavenumber and different boundary conditions on each end of the shell. Many researchers have studied the effects of boundary conditions on vibrations of circular cylindrical shells [15–20]. In order to evaluate the validity and accuracy of wave propagation, an exact solution for circular cylindrical shell with arbitrary boundary conditions is also obtained in the present study. The displacements of shell can be expressed as

$$\begin{aligned} u &= U_0 e^{\lambda x} \cos n\theta \cos \omega t, \\ v &= V_0 e^{\lambda x} \sin n\theta \cos \omega t, \\ w &= W_0 e^{\lambda x} \cos n\theta \cos \omega t. \end{aligned} \tag{8}$$

A characteristic equation about wavenumber $\lambda$ of order 8 can be derived following the similar procedure described above. For the usual range of shell parameters and $n \geqslant 1$, the eight roots of Eq. (8) have the form

$$\lambda = \pm\lambda_1, \quad \pm i\lambda_2, \quad \pm(\lambda_3 \pm i\lambda_4), \tag{9}$$

where $\lambda_i$ ($i = 1-4$) are real, positive numbers. The modal coefficients introduced as

$$\alpha_i = \frac{U_{0i}}{W_{0i}}, \quad \beta_i = \frac{V_{0i}}{W_{0i}}, \quad i = 1, 2, \ldots, 8 \tag{10}$$

These coefficients are calculated for these eight roots. Then, the displacements of shell can be rewritten as summation of these eight roots and corresponding modal coefficients. The characteristic matrix can be obtained after different boundary conditions having included [15],

$$[A]_{8\times 8}\{w_i\} = \{0\}, \quad i = 1, 2, \ldots, 8. \tag{11}$$

Expansion of the determinant of the above equation provides the system characteristic equation. Forsberg [15] and Warburton [16] presented different solving methods for this equation.

Three different boundary conditions of the circular cylindrical shell are studied in the present two approaches: they are shear SD–SD, C–C and C–SD. The wavenumber for wave propagation and boundary conditions of shell are listed in Table 1.

Nondimensional frequency parameter is defined as follows:

$$\Omega^2 = \frac{\rho(1-\nu^2)R^2}{E}\omega^2, \tag{12}$$

where $E$ is Young's modulus of elasticity, $\nu$ is the Possion ratio and $\rho$ is the density.

Table 1
Wavenumber and boundary conditions

| Boundary conditions of shell | Wavenumber | Displacement and force |
|---|---|---|
| Shear diaphragm–shear diaphragm (SD–SD) | $k_m L = m\pi$ | $v = w = N_x = M_x = 0, \quad x = 0, L$ |
| Clamped–clamped (C–C) | $k_m L = (2m+1)\pi/2$ | $u = v = w = \frac{\partial w}{\partial x} = 0, \quad x = 0, L$ |
| Clamped–shear diaphragm (C–SD) | $k_m L = (4m+1)\pi/4$ | $u = v = w = \frac{\partial w}{\partial x} = 0, \quad x = 0$ |
| | | $v = w = N_x = M_x = 0, \quad x = L$ |

## 3. Numerical results and discussion

A typical dispersion plot is given in Fig. 2a, b for a circular cylindrical shell with thickness ratio $h/R = 0.01$ and a circumferential modal number $n = 3$. Fig. 2b zooms in on the behavior of shell near the first cut-on frequency band. Only four roots are given in this plot for clarity.

When the driving frequency is very slow, Eq. (5) has eight conjugate roots. These eight roots can be divided into two groups. The two roots that have lower modulus firstly merge and transform into two purely imaginary ones (Point B1, Fig. 2b). Then one of these purely imaginary roots continues to grow and transforms to a purely real one as it crosses the axis, where the second root decreases. This 'two-phase' transformation occurs in a very narrow frequency band. With further growth in the driving frequency, two complex conjugate roots transform to two purely imaginary ones (Point B2, Fig. 2a). Thus, in the frequency range from approximately $\Omega = 1.08$ to 1.77 there exist one propagation wave and three evanescent waves. The second propagation wave is generated in a different manner, at $\Omega = 1.78$ a purely imaginary wavenumber become purely real. Even at this high frequency the wavelength of the propagating waves are much larger than the thickness of the shell so the thin shell theory is entirely applicable.

It should be noted that, the dispersion plot is continuous. With wave approach, discrete wavenumber is given according to various different boundary conditions. The corresponding resonant frequencies can be obtained from Eq. (5).

In order to evaluate the accuracy of the wave propagation, the results obtained here are compared with those from other researchers. Tables 2 and 3 are provided for 3 boundary conditions, respectively. In these tables, $m$ is the half number of circumferential waves of the vibration mode. Through comparison we can know that wave propagation is convenient and effective.

Two examples for comparison of frequency for a clamped–clamped cylindrical shell between FEM and wave propagation method are studied. The results are listed in Tables 4 and 5.

For the C–C boundary condition, the results from FEM are slightly lower than that of the wave propagation approach. However, the agreement for the lowest frequency is excellent.

In order to study the accuracy of wave propagation in detail, the results from wave propagation are compared with those from exact solution. A relative error parameter is defined as follows:

$$\text{Error}_P = \frac{P_{\text{wave}} - P_{\text{classical}}}{P_{\text{classical}}} \times 100\%, \tag{13}$$

which $P$ represents frequency, modal coefficients and wavenumbers. Subscript 'wave' and 'classical' represent the wave propagation method and the classical exact method, respectively.

Frequencies comparisons are given in Figs. 3–5. The relative error of wave propagation is smaller when the shell is longer. For given shell parameters, the relative error of SD–SD is the lowest among these three boundary conditions. A comparison for high vibration shape, $m = 2$, is given in Fig. 5. The frequencies error becomes small when $n$ increases.

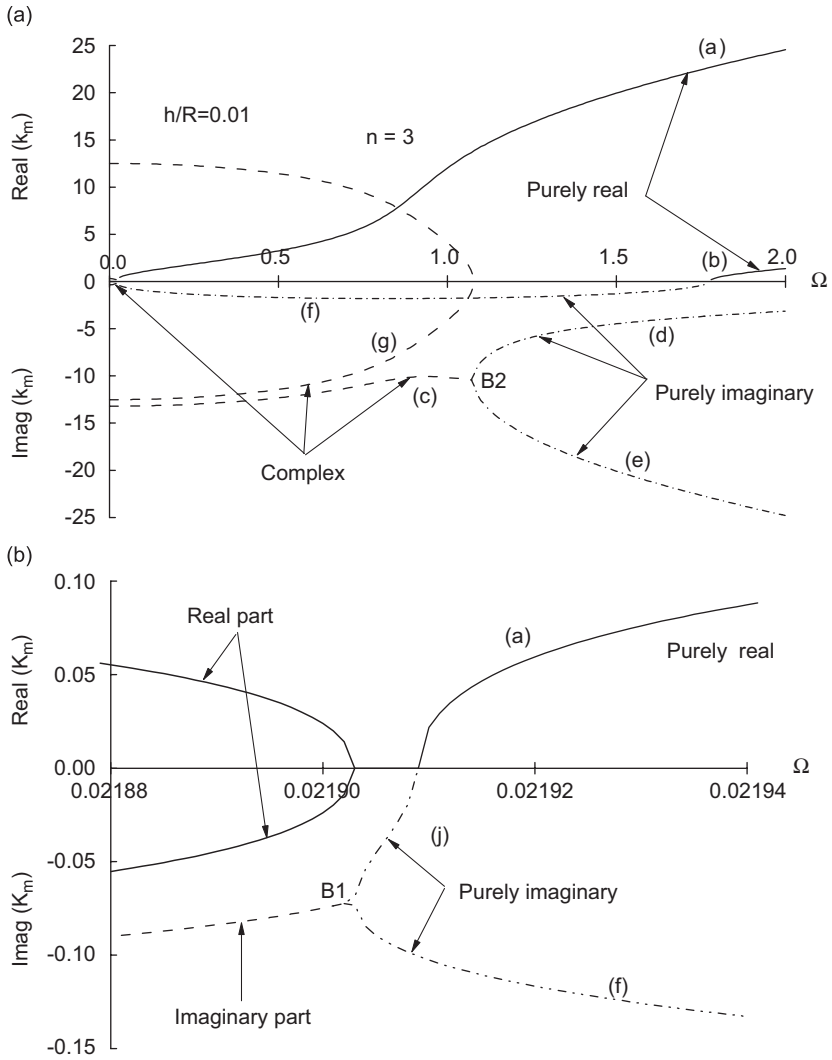


Fig. 2. (a) Dispersion plot for a circular cylindrical shell $h/R = 0.01$, $n = 3$. (b) A zoom view for lower frequency.

For short shells, the differences of frequencies between results obtained by the wave propagation method and the classical method are substantial. This is because the coupling between the circumferential and axial modes is ignored by using the beam function. The effects of this coupling are less important for long thin shells and for higher order modes such as shown in Fig. 4. The coupling effects between the circumferential and axial modes under clamped-shear diaphragm (C–SD) are less significant due to lack of constraints at one end. Thus, the differences of the axial mode coefficient of long shell for higher order are much higher as shown in Fig. 7.

The relative errors for shape coefficients are shown in Figs. 6–10. The errors are small when $n$ is small. When $n$ increases, the errors of axial shape become larger. This phenomenon is quite different from those in frequencies comparison. From these plots, we can also know that the error of axial displacement is larger than that of circumferential. Axial restraint has more effects on frequencies and shape coefficients of the shell. The more the restraints, the more the errors.

The errors of SD–SD are very small and can be neglected.

As can be seen from Eq. (5), the wavenumber will vary for different circumferential number $n$. But the wavenumber $k_m$ is assumed as a constant number during the wave propagation approach for given boundary conditions. This assumption will generate error certainly. In fact, beam is a one-dimensional structure.

Table 2
Comparison of values of the frequency parameter for $\Omega \times h\sqrt{2/(1-v)}/(\pi R)$ for a SD–SD shell $m = 1$, $h/R = 0.06$, $v = 0.3$

| $m\pi R/L$ | $n$ | $\Omega \times h\sqrt{2/(1-v)}/(\pi R)$ | | | | |
|---|---|---|---|---|---|---|
| | | Flügge [21] | Mirsky [22] | Bhimaraddi [21] | Lam and Loy [23] | Present |
| $0.5\pi$ | 1 | 0.01853 | 0.01853 | 0.01853 | 0.01853 | 0.01853 |
| | 2 | 0.01090 | 0.01090 | 0.01090 | 0.01089 | 0.01091 |
| | 3 | 0.00831 | 0.00829 | 0.00829 | 0.00828 | 0.00831 |
| | 4 | 0.01019 | 0.01011 | 0.01011 | 0.01018 | 0.01021 |
| $\pi$ | 1 | 0.02782 | 0.02781 | 0.02781 | 0.02787 | 0.02786 |
| | 2 | 0.02215 | 0.02214 | 0.02214 | 0.02217 | 0.02219 |
| | 3 | 0.01823 | 0.01818 | 0.01818 | 0.01823 | 0.01827 |
| | 4 | 0.01761 | 0.01748 | 0.01748 | 0.01761 | 0.01767 |
| $2\pi$ | 1 | 0.03717 | 0.03692 | 0.03692 | 0.03748 | 0.03739 |
| | 2 | 0.03644 | 0.03612 | 0.03612 | 0.03671 | 0.03666 |
| | 3 | 0.03610 | 0.03566 | 0.03566 | 0.03635 | 0.03634 |
| | 4 | 0.03695 | 0.03630 | 0.03632 | 0.03720 | 0.03723 |

Table 3
Comparison of values of the frequency parameter for $\Omega$ for a shell $m = 1$, $L/R = 20$, $h/R = 0.01$, $v = 0.3$ with C–C and C–SD boundary conditions

| $n$ | $\Omega$ | | | |
|---|---|---|---|---|
| | C–C | | C–SD | |
| | Zhang [6] | Present | Zhang [6] | Present |
| 1 | 0.034879 | 0.034879 | 0.024721 | 0.024722 |
| 2 | 0.014052 | 0.014052 | 0.011281 | 0.011281 |
| 3 | 0.022725 | 0.022726 | 0.022335 | 0.022335 |
| 4 | 0.042271 | 0.042272 | 0.042166 | 0.042166 |
| 5 | 0.068116 | 0.068116 | 0.068054 | 0.068055 |
| 6 | 0.099823 | 0.099823 | 0.099771 | 0.099772 |
| 7 | 0.137328 | 0.137329 | 0.137279 | 0.137280 |
| 8 | 0.180617 | 0.180618 | 0.180569 | 0.180569 |
| 9 | 0.229684 | 0.229684 | 0.229636 | 0.229636 |
| 10 | 0.284526 | 0.284527 | 0.284478 | 0.284478 |

Table 4
Comparison of values of the frequency (Hz) for a shell $L = 20\,\text{m}$, $R = 1\,\text{m}$, $h = 0.01\,\text{m}$, mass density $= 7850\,\text{kg/m}^3$, $E = 2.1 \times 10^{11}\,\text{N/m}^2$, $v = 0.3$, C–C boundary conditions

| Order | Modal shape ($m$,$n$) | FEM Zhang [6] | Wave propagation |
|---|---|---|---|
| 1 | 1,2 | 12.25 | 12.13 |
| 2 | 1,3 | 19.64 | 19.61 |
| 3 | 2,3 | 23.18 | 23.28 |
| 4 | 2,2 | 27.69 | 28.06 |
| 5 | 1,1 | – | 30.09 |
| 6 | 3,3 | 31.6 | 31.97 |
| 7 | 1,4 | 36.7 | 36.48 |
| 8 | 2,4 | 37.55 | 37.38 |
| 9 | 3,4 | 39.87 | 39.77 |

Table 5
Cylinder frequency comparison (Hz) for a shell $L = 0.8$ m, inside diameter $= 0.3048$ m, $h = 1.1016$ mm, $E = 64.73$ GPa, $v = 0.3285$, mass density $= 2700\,kg/m^3$ with C–C boundary conditions

| Wavenumber | | FEM [25] | Present |
|---|---|---|---|
| *m* | *n* | | |
| 1 | 1 | 1206.835 | 1643.599 |
| | 2 | 632.204 | 759.714 |
| | 3 | 368.149 | 406.966 |
| | 4 | 272.719 | 275.872 |
| | 5 | 290.999 | 296.349 |
| | 6 | 378.494 | 381.708 |
| | 7 | 504.107 | 506.585 |
| | 8 | 656.194 | 658.208 |
| | 9 | 831.114 | 832.645 |
| | 10 | 1027.733 | 1028.601 |
| 3 | 1 | 3423.025 | 3802.520 |
| | 2 | 2136.207 | 2464.041 |
| | 3 | 1397.860 | 1595.178 |
| | 4 | 976.570 | 1083.659 |
| | 5 | 744.515 | 801.741 |
| | 6 | 648.712 | 679.619 |
| | 7 | 661.399 | 679.018 |
| | 8 | 753.236 | 764.650 |
| | 9 | 897.792 | 906.315 |
| | 10 | 1078.946 | 1085.851 |
| 5 | 1 | – | 4568.875 |
| | 2 | 3384.730 | 3598.085 |
| | 3 | 2490.664 | 2703.534 |
| | 4 | 1861.695 | 2026.994 |
| | 5 | 1442.901 | 1557.579 |
| | 6 | 1181.739 | 1257.423 |
| | 7 | 1048.313 | 1097.372 |
| | 8 | 1023.828 | 1056.017 |
| | 9 | 1088.112 | 1110.359 |
| | 10 | 1219.158 | 1235.73 |

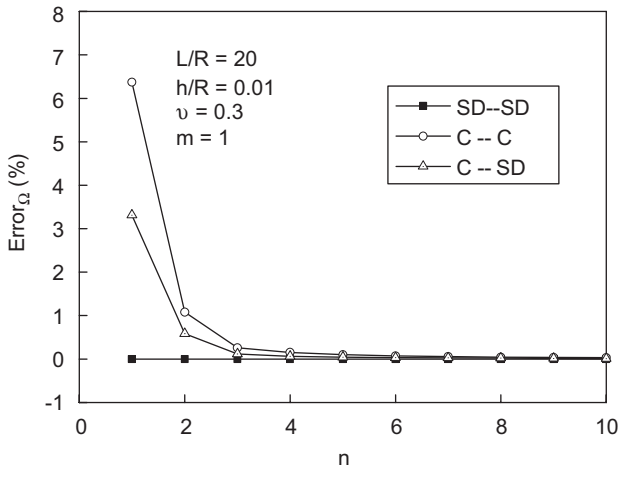


Fig. 3. Error curve for frequency parameter $L/R = 20$, $m = 1$.

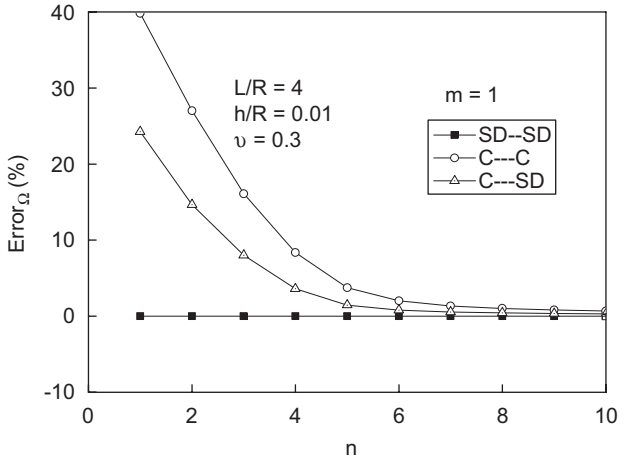


Fig. 4. Error curve for frequency parameter $L/R = 4$, $m = 1$.

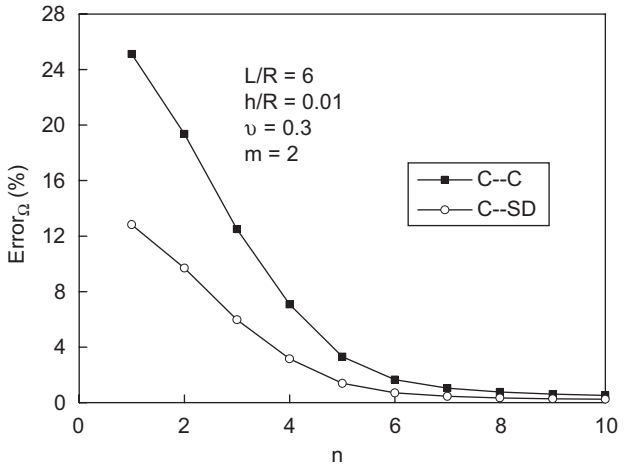


Fig. 5. Error curve for frequency parameter $L/R = 20$, $m = 2$.

Compared with beam, the wavenumber of shell should consider the effect of circumferential number. The wavenumber of shell is exactly equal to that of a beam only in the SD–SD boundary condition. Thus, it can be easily understood that the relative error of frequencies and the modal shape coefficients are quite small for SD–SD boundary conditions in the above comparisons. The errors of wavenumber are also examined in this present paper.

The comparisons for wavenumber of these two approaches are given in Fig. 11. In exact solution, the root $\lambda_2$ is chosen for comparison. $\lambda_2$ increases when $n$ become large, while the largest value is at $n = 4$, then $\lambda_2$ decreases. Relative error of wavenumber for a longer shell is given in Fig. 12. The error is much small when $n = 2$ and 3. The error increases quickly when $n$ increases. The clamped boundary condition has larger effects on relative error.

A further inspection into the wave propagation approach is given in Fig. 13 for comparison of the beam vibration mode ($m = 1$, $n = 1$) with that of a transverse vibration of beam. Fig. 13 shows a flexural wave in a flat plate, a torsional wave in a bar and an extensional wave in a flat plate. These three wave solutions are labeled (a), (b) and (c) respectively. The dispersion curve derived from the elementary Kirchhoff beam theory is displayed in thick black in this plot.

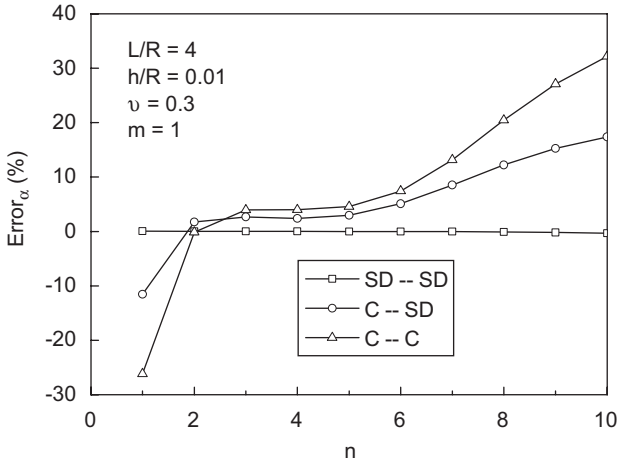


Fig. 6. Error curve of axial modal coefficient $L/R = 4$, $m = 1$.

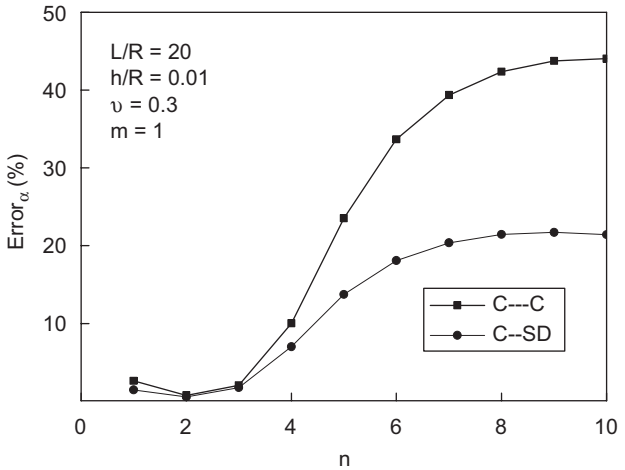


Fig. 7. Error curve of axial modal coefficient $L/R = 20$, $m = 1$.

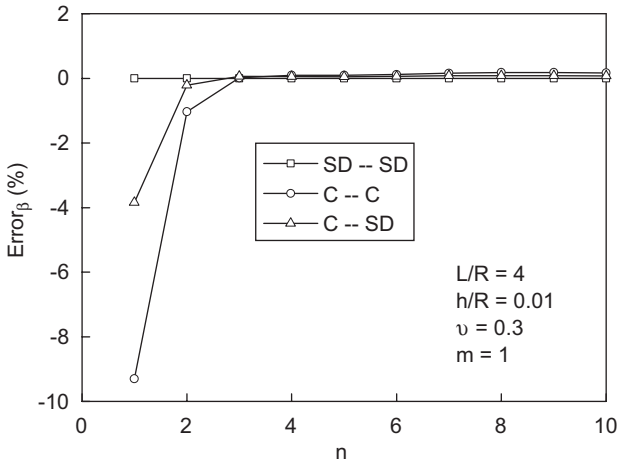


Fig. 8. Error curve of circumferential modal coefficient $L/R = 4$, $m = 1$.

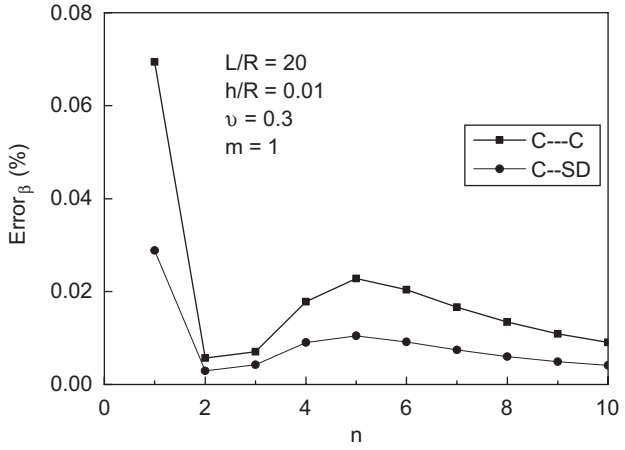


Fig. 9. Error curve of circumferential modal coefficient $L/R = 4$, $m = 1$.

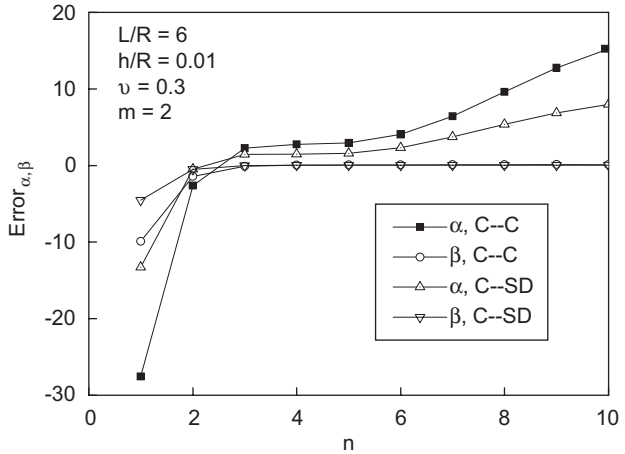


Fig. 10. Error curve of modal coefficient $L/R = 6$, $m = 2$.

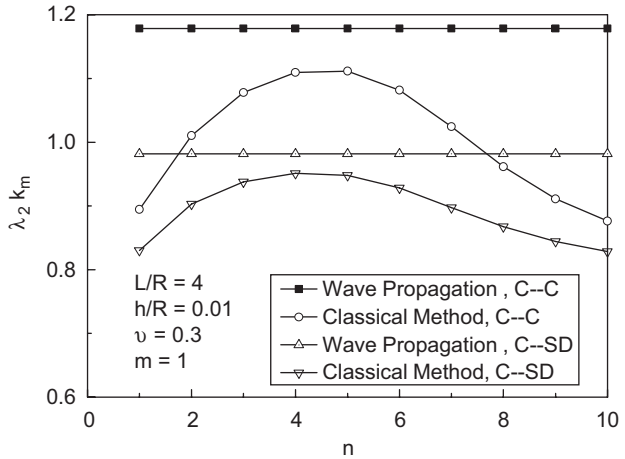


Fig. 11. Curves for wavenumber.

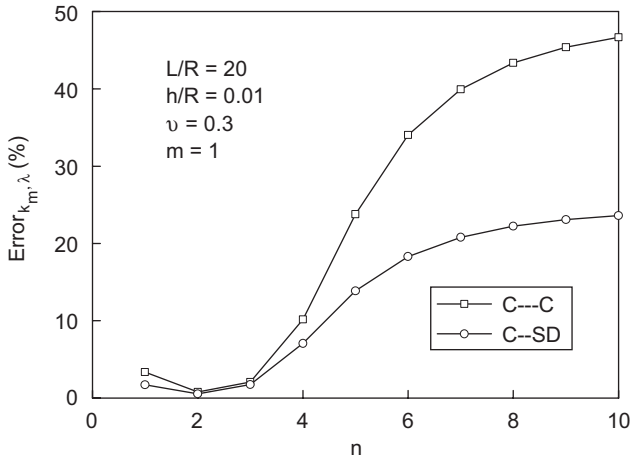


Fig. 12. Error curve for wavenumber.

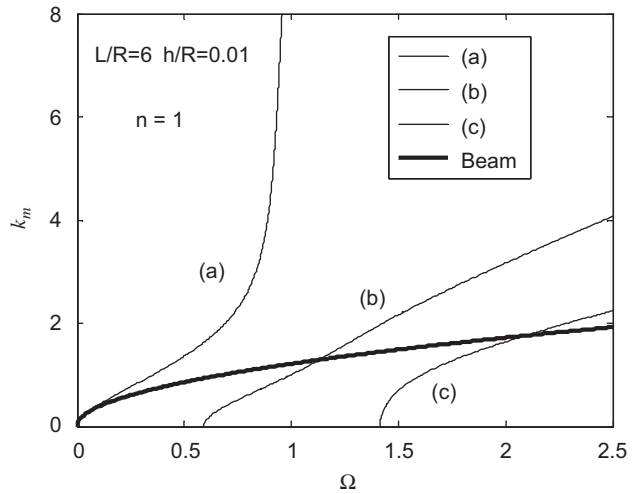


Fig. 13. Dispersion plot for beam mode $L/R = 6$, $h/R = 0.01$.

For a beam whose cross-section is a cylindrical shell tube of thickness $h$ and mean radius $R$, the area $A$ and inertia moment of cross-section $I$ are

$$A = 2\pi Rh, \quad I = \pi R^3 h\left(1 + \frac{h^2}{4R^2}\right). \tag{14}$$

The transverse vibration frequencies of a simply supported beam are

$$\omega_{\text{beam}}^2 = \frac{EI}{\rho A}\left(\frac{m\pi}{L}\right)^4, \quad \Omega_{\text{beam}}^2 = \frac{I(1-v^2)}{AR^2}(K_{m\text{-beam}}R)^4. \tag{15}$$

It can be seen from Fig. 13 that the beam curve is very close to that of the beam mode when the frequency is very small. This means, only when the shell is very long it is applicable to use beam theory to predict the frequency of shell.

## 4. Conclusions

The wave propagation approach and classical exact solution were applied to analyze the free vibration of circular cylindrical shell based on Flügge's classical thin shell theory in this study. The accuracy and validity of the wave propagation approach are studied, including comparisons for frequencies, vibration shapes and wavenumbers with those of exact solution. Some conclusions can be obtained from analysis.

Wave propagation is an efficient method for calculating the frequency of circular cylindrical shell. The wave propagation method has a high accuracy for a longer shell. In fact, so many researchers have used this method for analysis of pipe line (*in vacuo*, fluid-filled and submerged). This method also has very high accuracy of frequency, shape coefficient and wavenumber for SD–SD boundary conditions. In fact, the wavenumber in this boundary is exactly equal to that of the shell. Some relative errors will be introduced for those other than SD–SD boundary conditions.

## Appendix A

### *A.1. Differential operators $L_{ij}$*

$$L_{11} = R^2\frac{\partial^2}{\partial x^2} + (1+k)\frac{1-v}{2}\frac{\partial^2}{\partial\theta^2} - \frac{\rho h a^2}{D}\frac{\partial^2}{\partial t^2}, \quad L_{12} = \frac{1+v}{2}R\frac{\partial^2}{\partial x\partial\theta},$$

$$L_{13} = -vR\frac{\partial}{\partial x} + R^3k\frac{\partial^2}{\partial x^3} - \frac{1-v}{2}Rk\frac{\partial^3}{\partial x\partial\theta^2}, \quad L_{21} = \frac{1+v}{2}R\frac{\partial^2 u}{\partial x\partial\theta},$$

$$L_{22} = \left[\frac{1-v}{2}R^2 + \frac{3}{2}(1-v)R^2k\right]\frac{\partial^2}{\partial x^2} + \frac{\partial^2}{\partial\theta^2} - \frac{\rho h R^2}{D}\frac{\partial^2}{\partial t^2}, \quad L_{23} = \frac{3-v}{2}R^2k\frac{\partial^3}{\partial x^2\partial\theta} - \frac{\partial}{\partial\theta},$$

$$L_{31} = vR\frac{\partial}{\partial x} + \frac{1-v}{2}Rk\frac{\partial^3}{\partial x\partial\theta^2} - R^3k\frac{\partial^3}{\partial x^3}, \quad L_{32} = -\frac{3-v}{2}R^2k\frac{\partial^3}{\partial x^2\partial\theta} + \frac{\partial}{\partial\theta},$$

$$L_{33} = -(1+k) - R^4k\frac{\partial^4}{\partial x^4} - 2R^2k\frac{\partial^4}{\partial x^2\partial\theta^2} - k\frac{\partial^4}{\partial\theta^4} - 2k\frac{\partial^2}{\partial\theta^2} - \frac{\rho h R^2}{D}\frac{\partial^2}{\partial t^2},$$

$$D = \frac{Eh}{1-v^2}, \quad k = \frac{h^2}{12R^2}.$$

### *A.2. Elements of C matrix*

$$C_{11} = -R^2k_m^2 + \tfrac{1}{2}(1+k)(v-1)n^2 + \Omega^2, \quad C_{12} = -\tfrac{1}{2}\mathrm{i}nRk_m(1+v), \quad C_{13} = k(\mathrm{i}R^3k_m^3 + \tfrac{1}{2}\mathrm{i}n^2Rk_m(v-1) + \mathrm{i}Rk_mv),$$

$$C_{21} = -C_{12}, \quad C_{22} = \tfrac{1}{2}(-2n^2 + (1+3k)R^2k_m^2(v-1) + 2\Omega^2), \quad C_{23} = n - \tfrac{1}{2}knR^2k_m^2(-3+v),$$

$$C_{31} = -C_{13}, \quad C_{32} = C_{23}, \quad C_{33} = -1 - k(1+n^4 + R^4k_m^4 + 2n^2(-1+R^2k_m^2)) + \Omega^2.$$

### *A.3. The coefficients of Eq. (6)*

$$a_8 = \tfrac{1}{2}k(1-v)(k-1)(1+3k)R^8,$$

$$a_6 = -\tfrac{1}{4}kR^6(n^2(v-1)(-8+9k^2(v-1)+k(-11+3v))+2((2+6k)v^2-(3+k)\Omega^2+v(1+3k)(-2+\Omega^2))),$$

$$a_4 = -\frac{1}{4}R^4\begin{pmatrix} -2k(-4+6n^4(v-1)+4v+3v^2-3v^3+(3-7v)\Omega^2-2\Omega^4+n^2(6+9\Omega^2-3v(2+\Omega^2))) \\ +k^2(6-6v+6n^4(2-3v+v^2)+n^2(6v^3+v^2(\Omega^2-12)+6v(3+2\Omega^2)-3(4+3\Omega^2))) \\ +2k^3n^4(-1+v)v^2+2(v-1)(-1+v^2+\Omega^2) \end{pmatrix},$$

$$a_2 = -\frac{1}{4}R^2\begin{pmatrix} -2k(4n^6(-1+v)-2n^2(2+v^2+5\Omega^2+2\Omega^4-v(3+\Omega^2))+\Omega^2(6-3\Omega^2+v(3\Omega^2-4)) \\ +n^4(8+2v^2+9\Omega^2-v(10+3\Omega^2)))+k^2(n^6(7-10v+3v^2)+6(v-1)\Omega^2+n^4(v-1)(14+9\Omega^2+v(\Omega^2-10)) \\ -n^2(v-1)(7+9\Omega^2+v(-7+3\Omega^2)))+3k^3n^2(n^2-1)^2(v-1)^2+2\Omega^2(-3+2n^2(v-1)+v+2v^2+(3-v)\Omega^2) \end{pmatrix},$$

$$a_0 = \tfrac{1}{2}((1+k)(v-1)n^2+2\Omega^2)(k(-1+n^2)^2(n^2-\Omega^2)+\Omega^2(-1-n^2+\Omega^2)).$$

### A.4. The coefficients of Eq. (7)

$$b_6 = 1.0,$$

$$b_4 = \tfrac{1}{2}(-2-2n^2-2R^2k_m^2-2k(1+n^4+R^4k_m^4+2n^2(-1+R^2k_m^2))+(1+k)(v-1)n^2+(1+3k)(v-1)R^2k_m^2),$$

$$b_2 = \frac{1}{4}\begin{pmatrix} -2kn^6(-3+k(v-1)+v)-n^4(2k(5+3R^2k_m^2(v-3)-v)+2(v-1)+k^2(v-1)(-4+R^2k_m^2(9+v))) \\ -2R^2k_m^2\begin{pmatrix} (v-1)(3+R^2k_m^2+2v)+k^2(3(v-1)+R^4k_m^4(3v-1)+k(-6+R^4k_m^4(v-3)+4v+R^2k_m^2(-3+7v))) \\ -n^2\begin{pmatrix} 2k(-2R^2k_m^2(-5+v)+3R^4k_m^4(v-3)+2(v-2))+2(1+2R^2k_m^2)(v-1) \\ +k^2(2(v-1)-3R^2k_m^2(-3+2v+v^2)+R^4k_m^4(-9+12v+v^2)) \end{pmatrix} \end{pmatrix} \end{pmatrix},$$

$$b_0 = -\frac{1}{4}(v-1)\begin{pmatrix} 2R^4k_m^4(-1+v^2)-2k\begin{pmatrix} n^8+n^6(-2+4R^2k_m^2)+n^4(1+6R^4k_m^4+2R^2k_m^2(-4+v)) \\ +2n^2R^2k_m^2(2-3R^2k_m^2+2R^4k_m^4-v)+R^4k_m^4(4+R^4k_m^4-2R^2k_m^2v-3v^2) \end{pmatrix} \\ +k^3R^2k_m^2\left(6R^6k_m^6+3n^6(v-1)+3n^2\left(1+3R^4k_m^4\right)(v-1)+2n^4\left(3-3v+R^2k_m^2v^2\right)\right) \\ +k^2\begin{pmatrix} -2n^8+2n^4(-1+R^2k_m^2(7-5v)+3R^4k_m^4(v-2))-2R^4k_m^4(3+2R^4k_m^4-6R^2k_m^2v) \\ +n^6(4+R^2k_m^2(3v-7))+n^2R^2k_m^2(7(v-1)+R^4k_m^4(3v-11)+6R^2k_m^2(2-v+v^2)) \end{pmatrix} \end{pmatrix}.$$

### A.5. Elements of A matrix

Kirchhoff radial shear force $R_x = N_{x\theta} - (1/R)M_{x\theta}$ Kirchhoff membrane force $S_x = Q_x + (1/R)(\partial M_{x\theta}/\partial\theta)$. Elements of frequency determinant are

$$\begin{aligned}
&a_{11} = \alpha_1 e^{\lambda_1 x}, && a_{12} = -\alpha_1 e^{-\lambda_1 x}, && a_{13} = -\alpha_2 \sin \lambda_2 x, && a_{14} = \alpha_2 \cos \lambda_2 x, \\
&a_{15} = e^{\lambda_3 x}F_1, && a_{16} = e^{\lambda_3 x}F_2, && a_{17} = -e^{-\lambda_3 x}F_3, && a_{18} = e^{-\lambda_3 x}F_4, \\
&a_{21} = \beta_1 e^{\lambda_1 x}, && a_{22} = \beta_1 e^{-\lambda_1 x}, && a_{23} = \beta_2 \cos \lambda_2 x, && a_{24} = \beta_2 \sin \lambda_2 x, \\
&a_{25} = e^{\lambda_3 x}G_1, && a_{26} = e^{\lambda_3 x}G_2, && a_{27} = e^{-\lambda_3 x}G_3, && a_{28} = -e^{-\lambda_3 x}G_4, \\
&a_{31} = e^{\lambda_1 x}, && a_{32} = e^{-\lambda_1 x}, && a_{33} = \cos \lambda_2 x, && a_{34} = \sin \lambda_2 x, \\
&a_{35} = e^{\lambda_3 x} \cos \lambda_4 x, && a_{36} = e^{\lambda_3 x} \sin \lambda_4 x, && a_{37} = e^{-\lambda_3 x} \cos \lambda_4 x, && a_{38} = e^{-\lambda_3 x} \sin \lambda_4 x, \\
&a_{41} = \lambda_1 e^{\lambda_1 x}, && a_{42} = -\lambda_1 e^{-\lambda_1 x}, && a_{43} = -\lambda_2 \sin \lambda_2 x, && a_{44} = \lambda_2 \cos \lambda_2 x, \\
&a_{45} = e^{\lambda_3 x}H_1, && a_{46} = e^{\lambda_3 x}H_2, && a_{47} = -e^{-\lambda_3 x}H_3, && a_{48} = e^{-\lambda_3 x}H_4,
\end{aligned}$$

$$a_{51} = e^{\lambda_1 x}(\alpha_1\lambda_1 + vn\beta_1 - v + k\lambda_1^2), \qquad a_{52} = e^{-\lambda_1 x}(\alpha_1\lambda_1 + vn\beta_1 - v + k\lambda_1^2),$$
$$a_{53} = (-\alpha_2\lambda_2 + vn\beta_2 - v - k\lambda_2^2)\cos\ \lambda_2 x, \qquad a_{54} = (-\alpha_2\lambda_2 + vn\beta_2 - v - k\lambda_2^2)\sin\ \lambda_2 x,$$
$$a_{55} = e^{\lambda_3 x}(\lambda_3 F_1 - \lambda_4 F_2 + vnG_1 - v\cos\ \lambda_4 x + kI_1), \qquad a_{56} = e^{\lambda_3 x}(\lambda_3 F_2 + \lambda_4 F_1 + vnG_2 - v\sin\ \lambda_4 x + kI_2),$$
$$a_{57} = e^{-\lambda_3 x}(\lambda_3 F_3 - \lambda_4 F_4 + vnG_3 - v\cos\ \lambda_4 x + kI_3), \qquad a_{58} = e^{-\lambda_3 x}(-\lambda_3 F_4 - \lambda_4 F_3 - vnG_4 - v\sin\ \lambda_4 x + kI_4),$$
$$a_{61} = e^{\lambda_1 x}[+(1+3k)\beta_1\lambda_1 - n\alpha_1 - 3kn\lambda_1], \qquad a_{62} = e^{-\lambda_1 x}[-(1+3k)\beta_1\lambda_1 + n\alpha_1 + 3kn\lambda_1],$$
$$a_{63} = [-(1+3k)\beta_2\lambda_2 + n\alpha_2 + 3kn\lambda_2]\sin\ \lambda_2 x, \qquad a_{64} = [+(1+3k)\beta_2\lambda_2 - n\alpha_2 - 3kn\lambda_2]\cos\ \lambda_2 x,$$
$$a_{65} = e^{\lambda_3 x}[-nF_1 + (1+3k)(\beta_3 H_1 - \beta_4 H_2) - 3knH_1], \qquad a_{66} = e^{\lambda_3 x}[-nF_2 + (1+3k)(\beta_4 H_1 + \beta_3 H_2) - 3knH_2],$$
$$a_{67} = e^{-\lambda_3 x}[nF_3 + (1+3k)(\beta_4 H_4 - \beta_3 H_3) + 3knH_3], \qquad a_{68} = e^{-\lambda_3 x}[-nF_4 - (1+3k)(-\beta_4 H_3 - \beta_3 H_4) - 3knH_4],$$

$$a_{71} = e^{\lambda_1 x}\left[-\lambda_1^3 + (2-v)n^2\lambda_1 - \alpha_1\left(\lambda_1^2 + n^2\frac{1-v}{2}\right) - \frac{3-v}{2}\beta_1 n\lambda_1\right],$$

$$a_{72} = e^{-\lambda_1 x}\left[+\lambda_1^3 - (2-v)n^2\lambda_1 + \alpha_1\left(\lambda_1^2 + n^2\frac{1-v}{2}\right) + \frac{3-v}{2}\beta_1 n\lambda_1\right],$$

$$a_{73} = \left[-\lambda_2^3 - (2-v)n^2\lambda_2 + \alpha_2\left(-\lambda_2^2 + n^2\frac{1-v}{2}\right) + \frac{3-v}{2}\beta_2 n\lambda_2\right]\sin\ \lambda_2 x,$$

$$a_{74} = \left[\lambda_2^3 + (2-v)n^2\lambda_2 + \alpha_2\left(\lambda_2^2 - n^2\frac{1-v}{2}\right) - \frac{3-v}{2}\beta_2 n\lambda_2\right]\cos\ \lambda_2 x,$$

$$a_{75} = e^{\lambda_3 x}\left\{-(\lambda_3^2 - \lambda_4^2)H_1 + 2\lambda_3\lambda_4 H_2 + (2-v)n^2 H_1 - (\lambda_3^2 - \lambda_4^2)F_1 + 2\lambda_3\lambda_4 F_2 - \frac{3-v}{2}n(\beta_3 H_1 - \beta_4 H_2) - \frac{1-v}{2}n^2 F_1\right\},$$

$$a_{76} = e^{\lambda_3 x}\left\{-(\lambda_3^2 - \lambda_4^2)H_2 - 2\lambda_3\lambda_4 H_1 + (2-v)n^2 H_2 - (\lambda_3^2 - \lambda_4^2)F_2 - 2\lambda_3\lambda_4 F_1 - \frac{3-v}{2}n(\beta_4 H_1 + \beta_3 H_2) - \frac{1-v}{2}n^2 F_2\right\},$$

$$a_{77} = e^{-\lambda_3 x}\left\{-(\lambda_4^2 - \lambda_3^2)H_3 - 2\lambda_3\lambda_4 H_4 - (2-v)n^2 H_3 - (\lambda_4^2 - \lambda_3^2)F_3 - 2\lambda_3\lambda_4 F_4 - \frac{3-v}{2}n(\beta_4 H_4 - \beta_3 H_3) + \frac{1-v}{2}n^2 F_3\right\},$$

$$a_{78} = e^{-\lambda_3 x}\left\{-(\lambda_3^2 - \lambda_4^2)H_4 - 2\lambda_3\lambda_4 H_3 + (2-v)n^2 H_4 - (\lambda_3^2 - \lambda_4^2)F_4 - 2\lambda_3\lambda_4 F_3 - \frac{3-v}{2}n(\beta_4 H_3 + \beta_3 H_4) - \frac{1-v}{2}n^2 F_4\right\},$$

$$a_{81} = e^{\lambda_1 x}(\lambda_1^2 + \alpha_1\lambda_1 + vn\beta_1 - vn^2), \qquad a_{82} = e^{-\lambda_1 x}(\lambda_1^2 + \alpha_1\lambda_1 + vn\beta_1 - vn^2),$$
$$a_{83} = (-\lambda_2^2 - \alpha_2\lambda_2 + vn\beta_2 - vn^2)\cos\ \lambda_2 x, \qquad a_{84} = (-\lambda_2^2 - \alpha_2\lambda_2 + vn\beta_2 - vn^2)\sin\ \lambda_2 x,$$

$$a_{85} = e^{\lambda_3 x}[I_1 - vn^2\cos\ \lambda_4 x + \lambda_3 F_1 - \lambda_4 F_2 + vnG_1],$$
$$a_{86} = e^{\lambda_3 x}[I_2 - vn^2\sin\ \lambda_4 x + \lambda_3 F_2 + \lambda_4 F_1 + vnG_2],$$
$$a_{87} = e^{-\lambda_3 x}[I_3 - vn^2\cos\ \lambda_4 x + \lambda_3 F_3 - \lambda_4 F_4 + vnG_3],$$
$$a_{88} = e^{-\lambda_3 x}[I_4 - vn^2\sin\ \lambda_4 x - \lambda_3 F_4 - \lambda_4 F_3 - vnG_4],$$

where

$$
\begin{aligned}
&F_1 = \alpha_3 \cos \lambda_4 x - \alpha_4 \sin \lambda_4 x, && F_2 = \alpha_4 \cos \lambda_4 x + \alpha_3 \sin \lambda_4 x,\\
&F_3 = \alpha_3 \cos \lambda_4 x + \alpha_4 \sin \lambda_4 x, && F_4 = \alpha_4 \cos \lambda_4 x - \alpha_3 \sin \lambda_4 x,\\
&G_1 = \beta_3 \cos \lambda_4 x - \beta_4 \sin \lambda_4 x, && G_2 = \beta_4 \cos \lambda_4 x + \beta_3 \sin \lambda_4 x,\\
&G_3 = \beta_3 \cos \lambda_4 x + \beta_4 \sin \lambda_4 x, && G_4 = \beta_4 \cos \lambda_4 x - \beta_3 \sin \lambda_4 x,\\
&H_1 = \lambda_3 \cos \lambda_4 x - \lambda_4 \sin \lambda_4 x, && H_2 = \lambda_3 \sin \lambda_4 x + \lambda_4 \cos \lambda_4 x,\\
&H_3 = \lambda_3 \cos \lambda_4 x + \lambda_4 \sin \lambda_4 x, && H_4 = -\lambda_3 \sin \lambda_4 x + \lambda_4 \cos \lambda_4 x,\\
&I_1 = (\lambda_3^2 - \lambda_4^2)\cos \lambda_4 x - 2\lambda_3\lambda_4 \sin \lambda_4 x, && I_2 = (\lambda_3^2 - \lambda_4^2)\sin \lambda_4 x + 2e^{\lambda_3 x}\lambda_3\lambda_4 \cos \lambda_4 x,\\
&I_3 = (\lambda_3^2 - \lambda_4^2)\cos \lambda_4 x + 2\lambda_3\lambda_4 \sin \lambda_4 x, && I_4 = (\lambda_3^2 - \lambda_4^2)\sin \lambda_4 x - 2\lambda_3\lambda_4 \cos \lambda_4 x,
\end{aligned}
$$

## References


[1] W. Leissa, *Vibrations of Shells*, NASA SP 288, Washington, DC, 1973.
[2] C.R. Fuller, The effects of wall discontinuities on the propagation of flexural waves in cylindrical shells, *Journal of Sound and Vibration* 75 (2) (1981) 207–228.
[3] C.R. Fuller, F.J. Fahy, Characteristics of wave propagation and energy distributions in cylindrical elastic shells filled with fluid, *Journal of Sound and Vibration* 81 (4) (1982) 501–518.
[4] C.R. Fuller, The input mobility of an infinite circular cylindrical elastic shell filled with liquid, *Journal of Sound and Vibration* 87 (3) (1983) 409–427.
[5] C. Wang, J.C.S. Lai, Prediction of natural frequencies of finite length circular cylindrical shells, *Applied Acoustics* 59 (2000) 385–400.
[6] X.M. Zhang, G.R. Liu, K.Y. Lam, Vibration analysis of thin cylindrical shells using wave propagation approach, *Journal of Sound and Vibration* 239 (3) (2001) 397–403.
[7] X.M. Zhang, G.R. Liu, K.Y. Lam, Coupled vibration analysis of fluid-filled cylindrical shells using the wave propagation approach, *Applied Acoustics* 62 (2001) 229–243.
[8] X.M. Zhang, Frequency analysis of submerged cylindrical shells with wave propagation approach, *International Journal of Mechanical Science* 44 (2004) 1259–1273.
[9] X.M. Zhang, Vibration analysis of cross-ply laminated composite cylindrical shells using the wave propagation approach, *Applied Acoustics* 62 (2001) 1221–1228.
[10] M.B. Xu, X.M. Zhang, Vibration power flow in a fluid-filled cylindrical shell, *Journal of Sound and Vibration* 218 (4) (1998) 587–598.
[11] M.B. Xu, X.M. Zhang, W.H. Zhang, Space-harmonic analysis of input power flow in a periodically stiffened shell filled with fluid, *Journal of Sound and Vibration* 222 (4) (1999) 531–546.
[12] M.B. Xu, X.M. Zhang, W.H. Zhang, The effect of wall joint on the vibrational power flow propagation in a fluid-filled shell, *Journal of Sound and Vibration* 224 (3) (1999) 395–410.
[13] M.B. Xu, W.H. Zhang, Vibrational power flow input and transmission in a circular cylindrical shell filled with fluid, *Journal of Sound and Vibration* 243 (4) (2000) 387–403.
[14] W. Flügge, *Stresses in Shells*, Springer, New York, 1973.
[15] K. Forsberg, Influence of boundary conditions on the modal characteristics of thin cylindrical shells, *AIAA Journal* 2 (12) (1964) 2150–2157.
[16] G.B. Warburton, Vibration of thin cylindrical shells, *Journal of Mechanical Engineering Science* 7 (4) (1965) 399–407.
[17] W. Soedel, *Vibrations of Shells and Plates*, Marcel Dekker, New York, 1981.
[18] H. Chung, Free vibration analysis of circular cylindrical shells, *Journal of Sound and Vibration* 74 (3) (1981) 331–350.
[19] A. Ludwig, R. Krieg, An analytical quasi-exact method for calculating eigenvibrations of thin circular cylindrical shells, *Journal of Sound and Vibration* 74 (2) (1981) 155–174.
[20] J. Callahan, H. Baruh, A closed-form solution procedure for circular cylindrical shell vibrations, *International Journal of Solids and Structures* 36 (1999) 2973–3013.
[21] A. Bhimaraddi, A higher order theory for free vibration analysis of circular cylindrical shells, *International Journal of Solids and Structures* 20 (7) (1984) 623–630.
[22] I. Mirsky, G. Herrmann, Nonaxially symmetric motions of cylindrical shells, *Journal of Acoustical Society of America* 29 (1975) 1116–1124.
[23] K.Y. Lam, C.T. Loy, Effects of boundary conditions on frequencies of a multi-layered cylindrical shell, *Journal of Sound and Vibration* 188 (3) (1995) 363–384.
[24] A. Nosier, J.N. Reddy, Vibration and stability analyses of cross-ply laminated circular cylindrical shells, *Journal of Sound and Vibration* 157 (1992) 139–159.
[25] J.M. Santiago, H.L. Wisniewski, Convergence of finite element frequency prediction for a thin walled cylinder, *Computers and Structures* 32 (3/4) (1989) 745–759.